

HIGH RESOLUTION LONGITUDINAL PROPERTY MEASUREMENT USING EMITTANCE EXCHANGE BEAM LINE

Gwanghui Ha, Moohyun Cho, and Won Namkung, POSTECH, Pohang, Gyeongbuk 790-784, KOREA

Wei Gai, Kwang-Je Kim, and John Gorham Power, Argonne National Laboratory, Argonne, IL 60439, USA

Abstract

Most longitudinal diagnostics intentionally introduce a transverse-longitudinal correlation since it is difficult to measure longitudinal properties directly. This correlation is introduced in order to observe longitudinal properties on a transverse screen, but the initial transverse components of the beam limit the resolution of the measurement. It is possible to overcome this resolution limit with an emittance exchange beam line in which the transverse properties after the exchanger only depend on longitudinal properties at its entrance. We present a new concept for measuring longitudinal properties with an emittance exchange beamline and preliminary simulation results.

RESOLUTION LIMIT OF THE DEFLECTING CAVITY MEASUREMENT

Since it is difficult to measure the longitudinal density profile of an electron bunch directly, the longitudinal profile is often transformed into the transverse profile. An example is a transverse deflecting cavity (TDC) followed by a screen (Fig. 1). The TDC applies a time-dependent-transverse-kick to the bunch. The particles in the bunch obtain an additional transverse momentum depending on its arrival time at the TDC. Because the strength and the direction of this momentum kick varies with arrival time, the transverse position of each particle at the measurement screen is proportional to the longitudinal position inside the bunch. Therefore, we can estimate the bunch length by measuring the transverse beam size.

The transverse beam size at the screen downstream of the TDC (Fig. 1) is not an exact representation of the initial bunch length. The bunch's finite transverse size and divergence before the TDC contributes to the transverse beam size at the screen. To minimize the contribution of the initial transverse parameters, the quadrupole is used in front of the TDC. If all beam parameters at X_1 are well-known, then the beam size at the screen can be calculated using the linear transport matrix given in Eq. (1).

$$R = \begin{bmatrix} 1 & L_c + D + D' & \kappa \left(\frac{L_c}{2} + D \right) & 0 \\ 0 & 1 & k & 0 \\ 0 & 0 & 1 & 0 \\ \kappa & \frac{L_c}{2} \kappa & \frac{L_c}{4} \kappa^2 & 1 \end{bmatrix}, \quad (1)$$

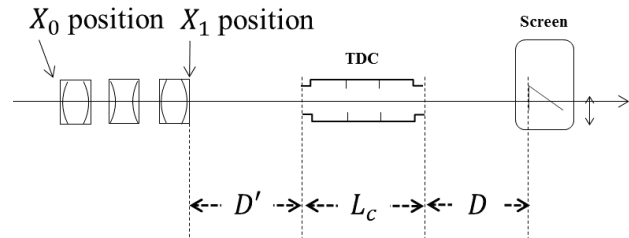


Figure 1: Typical TDC measurement configuration.

where κ is the deflecting cavity kick strength ($= \frac{eV}{E} \frac{2\pi}{\lambda}$).

According to Eq. (1), the rms transverse beam size at the screen position in terms of $X_1 = (x_1, x'_1, z_1, \delta_1)$ is

$$\sigma_{x,\text{screen}}^2 = \sigma_{x,1}^2 + L^2 \sigma_{x',1}^2 + 2L\sigma_{xx',1} + \kappa^2 L' \sigma_{z,1}^2. \quad (2)$$

where L is $L_c + D + D'$ and L' is $\frac{L_c}{2} + D$. The first three terms are due to the initial transverse parameters, while the last term is due to the bunch length. Two parameters from Eq. (2) determine the resolution. The first parameter, the scaling factor, determines the beam size at the screen due to the initial bunch length. Therefore, $\kappa L'$ in Eq. (2) is the scaling factor and a larger value improves the resolution. The second is the TDC-off transverse beam size. When the TDC is off, only the first three terms in Eq. (2) remain and the TDC-off size is the square root of those terms. The smaller the TDC-off size is the better the resolution.

To minimize the TDC-off size, the focal length of the quadrupole is adjusted to $\frac{1}{f} = -\left(\frac{1}{L} + \frac{\sigma_{xx',0}}{\sigma_{x,0}^2}\right)$ (a thin-lens single quadrupole is assumed for simple calculation instead of triplet). The corresponding minimum TDC-off size become

$$\sigma_{x,\text{min,screen}} = \frac{\epsilon_{x,0}}{\sigma_{x,0}} (D + D' + L_c). \quad (3)$$

The resolution of a TDC-based measurement is the ratio of the minimum TDC-off size to the scaling factor.

$$\text{Resolution} = \frac{\epsilon_{x,0}(D+D'+L_c)}{\sigma_{x,0}\kappa(D+\frac{L_c}{2})}. \quad (4)$$

Unfortunately, most of resolution related terms in Eq. (4) has a clear limit. A small emittance and large beam size enhance the resolution, but the emittance does not change

during the operation and the beam size cannot be larger than the diameter of beam pipe. D' and L_c have a minimum zero. D enhances the resolution up to certain point, but the terms in the bracket converge to the unity because D is on both the numerator and the denominator. The only remained factor which can keep enhancing the resolution is the cavity kick strength κ . However, since the resolution is the reciprocal of κ , increasing κ requires a large amount of RF power.

MEASUREMENT USING EMITTANCE EXCHANGE

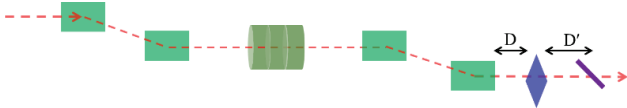


Figure 2: Schematics of the double dog-leg EEX beam line with an additional quadrupole for measurement of the longitudinal density profile.

The emittance exchange (EEX) beam line suggested in 2006 acts on the beam in a unique way [1]. The linear transport matrix of this beam line for $X = (x, x', z, \delta)$ is

$$R = \begin{bmatrix} 0 & 0 & \kappa L & \eta + \kappa \xi L \\ 0 & 0 & \kappa & \kappa \xi \\ \kappa \xi & \eta + \kappa \xi L & 0 & 0 \\ \kappa & \kappa L & 0 & 0 \end{bmatrix}. \quad (5)$$

This equation assumes the thin-lens deflecting cavity and the $1 + \kappa \eta = 0$ condition [1]. The unique characteristic of this matrix is zero diagonal block matrices, so that the upstream transverse and longitudinal properties cannot affect the downstream transverse and longitudinal properties respectively. Compared with a TDC-based measurement of the longitudinal profile, the transverse beam size at the exit is not affected by the initial transverse beam size. This transverse beam size at the exit only depends on the initial bunch length and the energy spread. If we tune the EEX beamline to zero R_{13} or R_{14} , then the initial bunch length or the energy spread would have a linear relation with the final transverse beam size.

It is possible to make R_{13} or R_{14} zero by introducing an additional quadrupole as shown in Fig. 2. To measure the longitudinal profile, the focal length of the quadrupole can be set to $f_z = -\frac{D'(\eta + \kappa \xi(L+D))}{\kappa \xi D' + \eta + \kappa \xi(L+D)}$, and the first row of Eq. (5) becomes

$$\begin{bmatrix} 0 & 0 & \frac{\eta \kappa}{\eta + \kappa \xi(L+D)} D' & 0 \end{bmatrix}. \quad (6)$$

Similarly, to measure the energy spread the focal length of the quad is set to $f_E = -\frac{D'(L+D)}{L+D+D'}$ and the first row of Eq. (5) becomes

$$\begin{bmatrix} 0 & 0 & 0 & -\frac{\eta}{L+D} D' \end{bmatrix}. \quad (7)$$

Since EEX with a single quadrupole provides a linear relation between the final horizontal beam size and the one of the initial longitudinal properties. Therefore, the resolution for the bunch length and the energy spread can be improved by increasing the kick from the TDC (κ) and the drift length D' respectively.

COMPARISON OF TDC AND EEX RESOLUTION

To compare both methods for longitudinal profile measurement, we prepare the beam line and input beam parameters for the EEX method (Table 1). For the TDC method, the resolution is calculated by Eq. (2), (3), and (4). κ is the same as the number in Table 1. D' and L_c are set to zero to achieve the best resolution. D is 15 m which is close to the total length of EEX method. For the input beam condition, the same numbers in Table 1 is used.

Table 1: Beam and Beam Line Parameters for Simulation

Beam line parameter	Value	Unit
Bending angle	5.00	deg
Dipole-to-Dipole distance	5.00	m
Dipole-to-TDC distance	0.20	m
η (dispersion of dog-leg)	-0.46	m
ξ (momentum compaction of dog-leg)	0.04	m
κ (TDC kick strength)	2.15	m^{-1}
Input beam parameter	Value	Unit
Beam size	0.1	mm
Transverse emittance	0.1	μm
Bunch length	1	fs
Energy spread	0.1	%

According to Eq. (4), the resolution of this system is $5.8 \mu m$ (≈ 20 fs) which is much larger than the initial rms bunch length of 1 fs. Compare to the calculated intrinsic size of $187 \mu m$, the product of the initial bunch length and

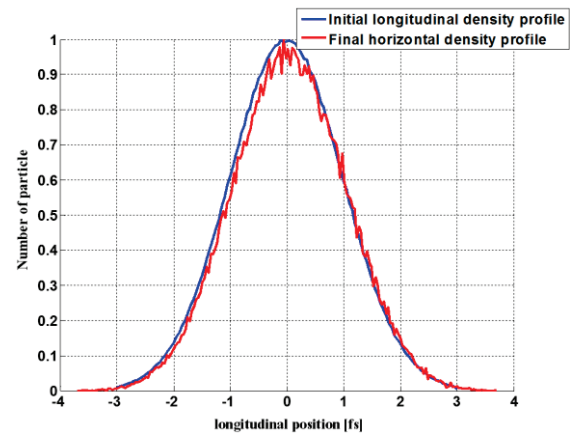


Figure 3: The longitudinal density profile before the EEX (blue) and the reconstructed longitudinal density profile from the horizontal density profile after the quadrupole (red).

Content from this work may be used under the terms of the CC BY 3.0 licence (© 2015). Any distribution of this work must maintain attribution to the author(s), title of the work, publisher, and DOI.

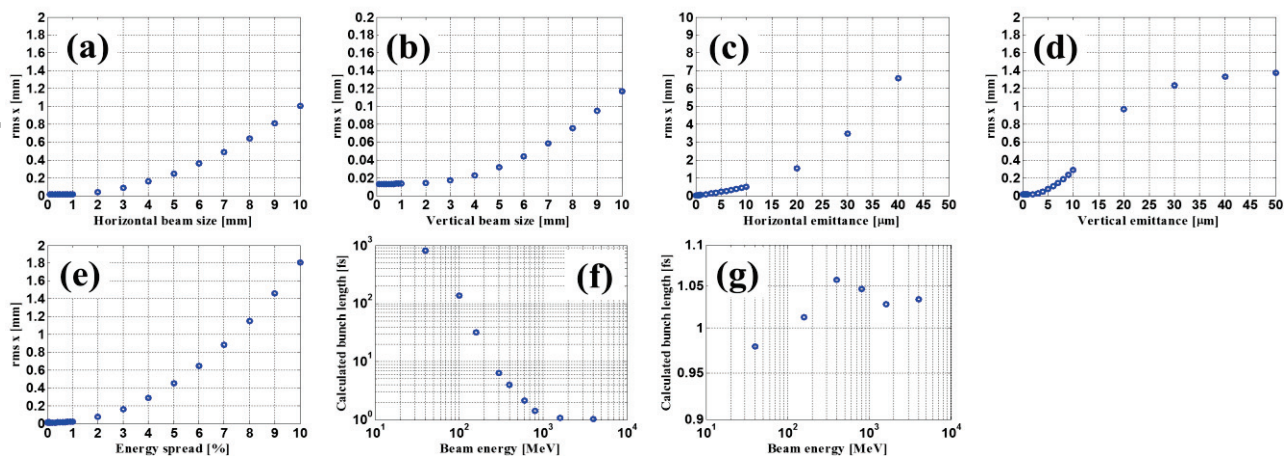


Figure 4: Rms horizontal beam size at the screen after EEX and quad as function of input beam parameters for an initial rms bunch length of 1fs. Collective effects are ignored for (a)-(e). Space-charge effect is considered for (f) and CSR is considered for (g).

the scaling factor gives only 9.6 μm . Therefore, the TDC-based method is not compatible with this beam conditions.

The EEX method was simulated using General Particle Tracer (GPT) [2]. Collective effects are turned off for comparison to the analytic treatment of the TDC-based method given above. Fig. 3 shows the reconstructed longitudinal density profile from the EEX method which is in a good agreement with the initial longitudinal density profile in the case where the initial bunch length is 1 fs.

LIMITING EFFECTS

Figure 4 shows the horizontal beam size at the screen for different input beam conditions but fixed input bunch length of 1 fs. The beam line parameters and the input beam parameters in Table 1 were used to observe the limiting effects. To explore the second order effects, the collective effects were turned off. To study the collective effects, GPT's 3D space-charge routine and CSR routine [3] were used. For the simulations, initially upright 6D Gaussian distribution with Table 1 parameters was generated at the entrance, and the parameter related to the limiting effects was varied.

For the upright ellipse distribution, T111, T122, T133, T144 and T166 produced second order effects in the double dog-leg EEX beam line. Fig. 4 (a)-(e) show two different trends based on the magnitude of the input beam parameter. When the parameters were less than 1 mm for the beam size, 1% for the energy spread and 5 μm for the emittance, the rms beam size at the screen does not change. This means that there is no linear relation between these parameters and the final horizontal position. In the case of the horizontal emittance, the graph shows a linear relation when the emittance is small. This is due to the thickness of the TDC [1] which can be cancelled with an additional accelerating cavity [4]. As the parameters increase further, quadratic dependence become apparent due to the second order terms. The EEX method for longitudinal diagnostics is not useful when the input beam parameters are in this range.

Figure 4 (f) and (g) consider collective effects. For the simulation, a charge of 100 pC was used while the beam energy was varied. Since the bending angle is only five degrees, CSR was not a significant effect as can be seen in Fig. (g). Based on this observation, reducing the bending angle can be a good solution for both the second order effect and the CSR, but this low bending angle also reduces the dispersion ($= 1/\kappa$), in which increases the required RF power for the TDC. For the parameters in Table 1, the space charge effect is the dominant effect changing the beam size. At 40 MeV, the space charge changes the beam size from 10 μm to 10 mm. According to Fig. 4 (f), beam energy should be more than 1 GeV to suppress this space charge effect.

CONCLUSION

We presented a new method for measure the longitudinal profile with high resolution. This method provides very high resolution for normal levels of bunch length and energy spread. Also, it is capable of measuring sub-fs long bunch length, which is hard to measure using the TDC-based method which is limited by the intrinsic beam size. We also determined the limiting effects of this new method which can be large depending on the input beam conditions. We have shown that this double dog-leg EEX beam line has excellent resolution within a limited range of the input beam conditions. In the future, we will explore how to extend this method to a broader set of input beam conditions.

REFERENCES

- [1] P. Emma et al., Phys. Rev. ST Accel. Beams 9, 100702 (2006).
- [2] www.pulsar.nl/gpt
- [3] I. V. Bazarov et al., "Calculation of coherent synchrotron radiation in General Particle Tracer", Proc. EPAC2008, Genoa, Italy, pp. 118 (2008), <http://jacow.org/>
- [4] A. A. Zholents et al., ANL-APS-LS-327, (2011).